Baltic Astronomy, vol. 15, 269–274, 2006.

SEARCHING FOR OBSERVATIONAL EVIDENCE OF TIDALLY INCLINED PULSATIONS

M. D. Reed[1] and the Whole Earth Telescope Xcov 21 and 23 collaborations[2]

[1] *Missouri State University, Springfield, MO 65804, U.S.A.*

[2] *Complete lists of participants available at wet.physics.iastate.edu*

Received 2005 August 1

Abstract. We attempt to interpret frequencies detected in KPD 1930+2752 with those of a pulsator in which the pulsation axis is influenced by tidal forces and continually points toward the companion. KPD 1930+2752 is in a close binary with a period of about 2 hours. It was observed by the Whole Earth Telescope in the summer of 2003.

Key words: stars: post-AGB – stars: oscillations – stars: individual (KPD 1930+2752)

1. INTRODUCTION

In order for asteroseismology to discern the internal conditions of variable stars, the pulsation "mode" as represented mathematically by spherical harmonics with quantum numbers n (sometimes designated k), ℓ and m, must be identified. For nonradial, multimode pulsating stars, pulsation periods, frequencies and/or the spacings between them are used to discern the spherical harmonics (see for example Winget et al. 1991). These *known* modes are then matched to models that are additionally constrained by non-asteroseismic observations; typically $T_{\rm eff}$ and $\log g$ from spectroscopy. Within such constraints, the model that most closely reproduces the observed pulsation periods (or period spacing) for the proper modes is inferred to be the correct one. Occasionally, such models can be confirmed by independent measurements (Reed et al. 2004; Reed, Kawaler & O'Brien 2000; Kawaler 1999). Unfortunately, more often than not, it is impossible to uniquely identify the spherical harmonics and asteroseismology cannot be applied to obtain a unique conclusion.

Several methods are being pursued to observationally constrain the spherical harmonics including time-series spectroscopy (see Telting et al. 2006, Aerts et al. 2006, Harms et al. 2006, Schoenaers & Lynas-Gray 2006 and Geier et al. 2006 in these proceedings) and multicolor photometry (see Jeffery et al. 2006). Our contribution is to use tidal forces in close binaries.

Analogous to the oblique pulsator model described by Kurtz (1992), that has been successfully applied to roAp stars, tidal forces may impact pulsations by inclining the spherical harmonics towards the companion along the tidal force. KPD 1930+2752 (hereafter KPD 1930) was discovered to be an sdBV star with a massive white dwarf companion in a 2.5 hour binary (Billères et al. 2001). In this

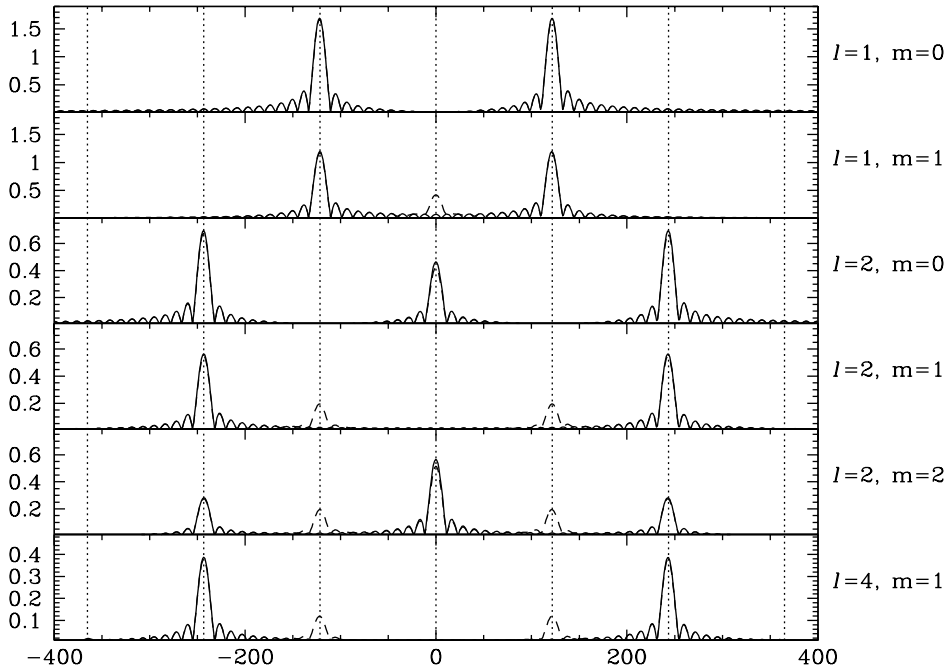

Fig. 1. Temporal spectra (Fourier transform, FT) of simulations for KPD 1930 assuming a tidally induced pulsation axis. The solid lines are simulations for an orbital axis of 90° and the dashed lines are for an orbital axis of 80°. The dotted lines indicate the input frequency (at 0) and orbital splittings.

case the tidal force is strong enough to slightly distort the sdB star but no eclipses have been positively detected. As the pulsation geometry should align with the strongest force, a measure of the likelihood of the pulsation axis to point at the companion is the ratio of the tidal to centrifugal acceleration. For KPD 1930 this ratio is 1.7:1, making it the best candidate known at this point.

2. WHAT DO WE EXPECT TO SEE?

We have previously discussed our simulations to determine the impact on pulsations for a pulsation axis that points at the companion and precesses with the orbital period (Reed, Brondel & Kawaler 2005; Reed et al. 2001). For KPD 1930 we can specifically ask what we expect to see. Our simulations calculate the relative brightness for a grid of 10 000 points on the observable surface of the star (one half of the entire spherical surface with the line-of-sight remaining constant). A modest amount of limb darkening was included using limb darkening coefficients from van Hamme (1993) for a model with $T_{\rm eff} = 29\,000$ K and $\log g = 5.0$ for the square root law at $\lambda = 5000$ Å. For the simulations in this paper, we used pulsation and orbital periods appropriate for KPD 1930, assuming that the tidal force causes the pulsation axis to point directly at the companion and tested two orbital (rotational) axis inclinations of 80° and 90°. Figure 1 shows the results of these

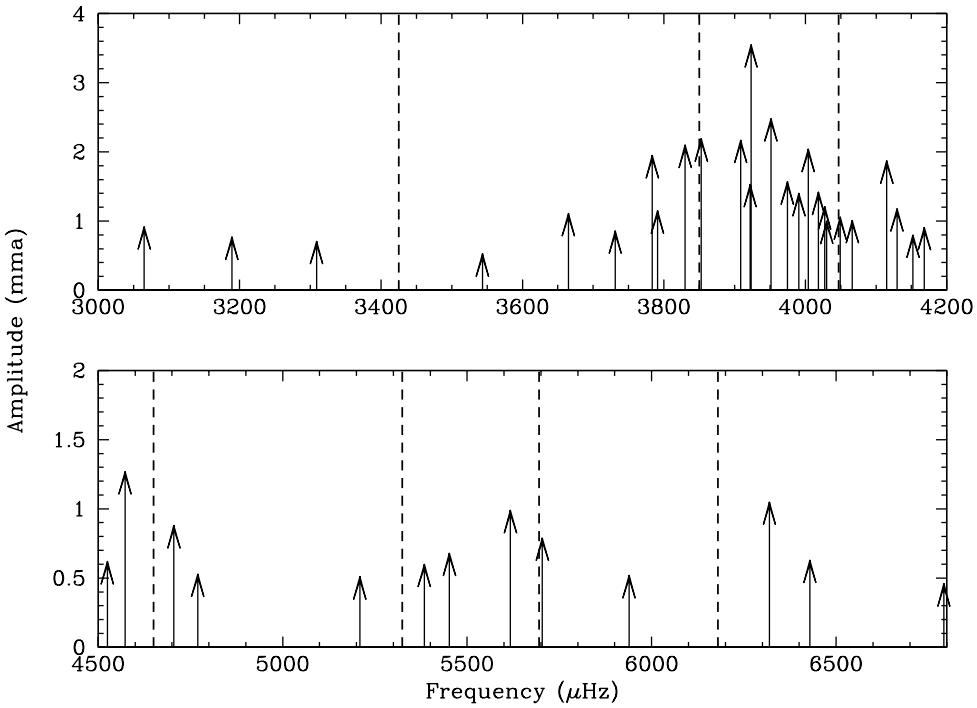

Fig. 2. Representation of the temporal spectrum (FT) for KPD 1930. Arrows indicate frequencies detected with the height indicating the observed amplitude. Dashed lines indicate frequencies we anticipate to detect once the data are divided into phases appropriate for various modes.

simulations for several pulsation modes. For each panel of the figure, we input a single frequency (at 0 μHz) and then, using 10 s time steps, integrated the light curve over about 10 orbital cycles (about a day). This has been done for two inclinations for the binary/rotation axis: 80° (dashed lines in the figure) and 90°. As the dashed 80° lines are nearly indistinguishable from the solid 90° lines, we can conclude that small changes in the binary/rotation axis will not change the results. Note that in four of the six modes shown, the original, input frequency is not detected. This is because the phase of pulsation changes over the orbital period as we "look" at opposite sides of the star. These opposite phases serve to cancel the input frequency in many cases. If the light curve is properly divided into regions of like phase for an individual pulsation mode, the central, input frequency is recovered. So even though both of the m values for $\ell = 1$ look the same, the data are divided differently to recover the input frequency. As such, different m values are easily distinguishable.

2.1. The pulsation content of KPD 1930

The next step is to examine the observed frequency content of KPD 1930 in the complete data set to look for multiplets matching those in Figure 1. An examination of the complete frequency content of KPD 1930 is beyond the scope (and

Table 1. Pulsation frequencies split by a multiple of the rotation/orbital frequency. The pulsation frequencies are in descending order and the number in parentheses indicates the multiple of the rotation/orbital frequency between itself and the previously listed frequency.

6791.9:	6428.9 (3), 5938.6 (4), 5451.8 (4), 5208.9 (2)
5383.8:	4769.8 (5), 4524.8 (2)
4705.2:	3974.5 (6), 3852.7 (1), 3731.1 (1)
4168.1:	4049.2 (1), 3923.2 (1)
4152.1:	4030.2 (1), 3908.5 (1), 3783.4 (1), 3664.9 (1), 3543.2 (1), 3308.8 (2),
cont.	3188.9 (1), 3064.9 (1)
4129.6:	4004.0 (1)
4115.0:	3990.8 (1)
4066.4:	3951.2 (1), 3829.9 (1)
3921.9:	3790.9 (1)

space) of this paper, but 39 frequencies have been detected with some confidence in the Xcov 23 data. Table 1 lists those frequencies which form multiplets near the orbital/rotational frequency splitting. The pulsation frequencies are listed in descended order (an arbitrary choice) with the multiple of the splitting between that frequency and the previously listed one in parentheses.

Anytime we see a splitting of $2 \times f_{\rm orb}$, it is an indication of a tipped $\ell = 1$ mode, while splittings of $4 \times f_{\rm orb}$ indicate either an $\ell\, m = 2, 1$ or $4, 1$ mode. Figure 2 shows arrows representing frequencies detected in the Xcov 23 data, and the dashed lines indicate where we would expect new peaks to appear when the data are phase-separated for individual modes.

3. WHAT DO WE REALLY SEE?

Now that we know what to potentially look for from the simulations, and where to look for new peaks from the complete data set, it is time to separate the data into regions of like phases for various pulsation modes and see what appears. Pulsations modes that would change phases during an orbital cycle are separated so that all the data for each phase forms a data set. Then we can fit and prewhiten them in the usual manner, without influence from the complete data set (that is, reduce them as per normal without assuming any a priori frequencies). Frequencies that match between the two phase sets are then examined to see if they (1) are detected in the complete data or are only in the phased data, (2) at a frequency expected (dashed lines in Figure 2) if not in the complete data, and/or (3) differ in phase as expected. Figures 3 and 4 show data phase-separated for several different pulsation modes.

4. RESULTS

We have examined data from Xcov 23 to look for indications of tidally modified pulsations. As can be seen from Figures 3 and 4, we have failed to detect any. No new frequency peaks appear where we would expect them to. Though KPD 1930 is the best candidate for such inclined pulsations to occur, our efforts have been thwarted by an incredibly rich and complex pulsation spectrum. KPD 1930 has at least 39 independent pulsation frequencies, perhaps many more,

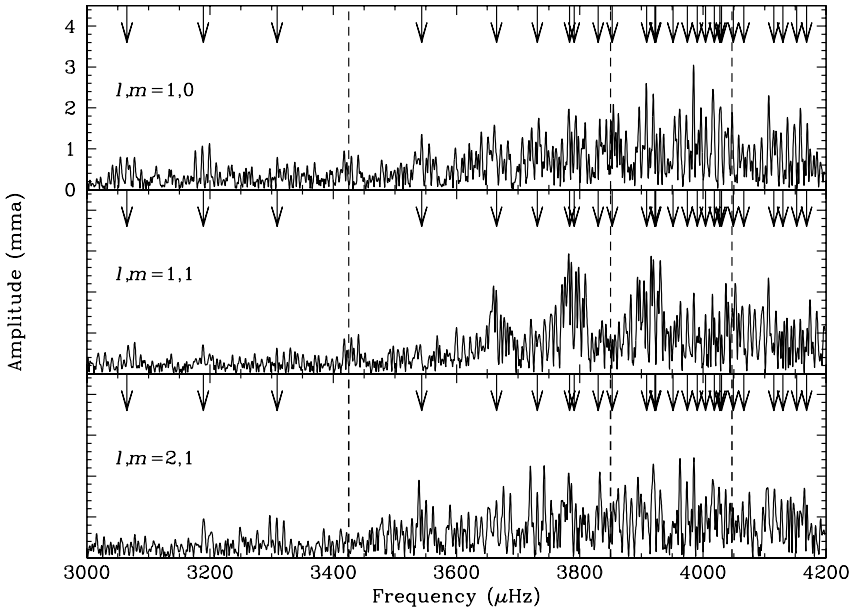

Fig. 3. Temporal spectra of Xcov 23 data separated appropriately for phase for the given mode. Only one of the phases is shown. The arrows and dashed lines are the same as in Fig. 2 except the arrows are inverted.

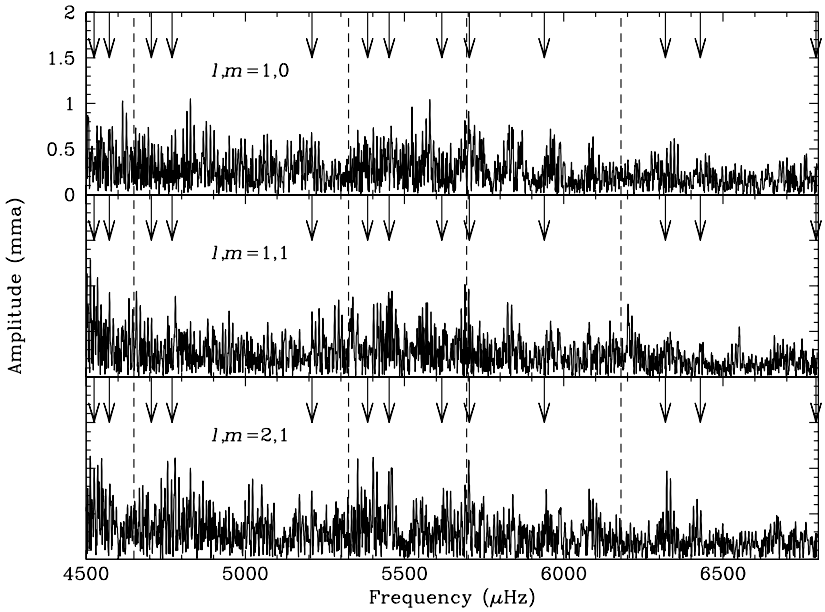

Fig. 4. The same as Fig. 3 for the higher frequency range.

with the amplitudes changing over just a few days. As such, it is incredibly difficult

to interpret. If the data are divided such that amplitudes of pulsations are roughly constant, then most of the frequencies are unresolved. If the data are long enough to resolve the pulsations, then the amplitudes have changed significantly within the data set, perhaps even disappearing altogether. It seems that if it is at all possible to understand the pulsation nature of KPD 1930, it will require constant, single-instrument observations over several weeks. Satellites such as MONS (which will not observe KPD 1930) would be the tool of choice. For such a complex pulsator, any additional complications, such as those from multiple and multiply-sensitive instruments, or aliasing caused by gaps in the data, make the temporal spectrum impossible to decipher.

ACKNOWLEDGMENTS. This material is based in part upon work supported by the National Science Foundation under Grant Numbers AST 007480 and AST 9876655. Any opinions, findings and conclusions or recommendations expressed in this material are those of the author(s) and do not necessarily reflect the views of the National Science Foundation.

REFERENCES

Aerts C., Jeffery C. S., Dhillon V. S. et al. 2006, Baltic Astronomy, 15, 275 (these proceedings)

Billéres M., Fontaine G., Brassard P., Charpinet S., Liebert J., Saffer R. A., Bergeron P., Vauclair G. 1998, ApJ, 494, L75

Geier S., Heber U., Przybilla N., Kudritzki R.-P. 2006, Baltic Astronomy, 15, 243 (these proceedings)

Harms S., Reed M. D., O'Toole S. J. 2006, Baltic Astronomy, 15, 251

Jeffery C. S., Aerts C., Dhillon V. S., Marsh T. R. 2006, Baltic Astronomy, 15, 259 (these proceedings)

Jeffery C. S., Pollacco D. 2000, MNRAS, 318, 974

Kawaler S. D. 1999, in *The 11th European White Dwarf Workshop*, ed. J.-E. Solheim, ASP Conf. Ser., 158, 169

Kurtz D. W. 1992, MNRAS, 259, 701

Reed M. D., Brondel B. J., Kawaler S. D. 2005, ApJ, accepted

Reed M. D. et al. 2004, MNRAS, 348, 1164

Reed M. D., Kawaler S. D., O'Brien M.S. 2000, ApJ, 545, 429

Reed M. D., Kawaler S. D., Kleinman S. J. 2001, in *12th European Workshop on White Dwarfs*, eds. J. L. Provencal, H. L. Shipman, J. MacDonald & S. Goodchild, ASP Conf. Ser. 226, 181

Schoenaers C., Lynas-Gray A. E. 2006, Baltic Astronomy, 15, 219 (these proceedings)

Telting J., Østensen R. H., Heber U., Augusteijn T. 2006, Baltic Astronomy, 15, 235 (these proceedings)

van Hamme W. 1993, AJ, 106, 2096

Winget D. E. et al. 1991, ApJ, 378, 326